Clinical Interventions in Aging

Dovepress
Taylor & Francis Group

Open Access Full Text Article

ORIGINAL RESEARCH

A Machine Learning Model Integrating Systemic Immune-Inflammation Index for Predicting 28-Day Mortality in Geriatric Sepsis Secondary to Community-Acquired Bacterial Pneumonia

Yifei Xu, Wei Chen

Department of Intensive Care Unit, Beijing Shijitan Hospital, Capital Medical University, Beijing, People's Republic of China

Correspondence: Wei Chen, Department of Intensive Care Unit, Beijing Shijitan Hospital, Capital Medical University, No. 10, Tieyi Road, Haidian District, Beijing, 100038, People's Republic of China, Email hanwa63@126.com

Purpose: Sepsis is a life-threatening clinical syndrome characterized by a dysregulated host response to infection. The systemic immune-inflammation index (SII) is a novel prognostic biomarker, However, its predictive value for early prognosis in elderly individuals suffering from sepsis secondary to community-acquired bacterial pneumonia (CABP) remains unclear. This study intends to apply machine learning techniques to develop an interpretable model for predicting prognosis.

Patients and Methods: This medical records review included elderly patients with sepsis secondary to CABP admitted to ICUs at Beijing Shijitan Hospital. Clinical outcomes based on 28-day survival status served as the basis for dividing participants into survivor and non-survivor groups. For prognostic prediction, five machine learning algorithms were developed, including Gradient Boosting Machine (GBM), Logistic Regression, Random Forest (RF), Light Gradient Boosting Machine (LightGBM), and Extreme Gradient Boosting (XGBoost). Model efficacy was quantified using the area under the receiver operating characteristic curve (AUROC) metric and assessed clinically through decision curve analysis (DCA). SHapley Additive exPlanations (SHAP) visualization provided insights into the models' decision-making processes.

Results: In this investigation, clinical information from 364 geriatric participants suffering from sepsis secondary to CABP was examined. For developing prediction models, twelve predictors were chosen. During an extensive evaluation of multiple computational frameworks, the XGBoost algorithm exhibited superior prognostic capability regarding 28-day mortality (AUROC = 0.901, 95% CI: 0.853−0.949,). The SHAP summary plot generated from the optimal XGBoost model ranked the importance of predictive features. The SII, APACHE II score, age, Pneumonia Severity Index (PSI), gender was identified as the top five most influential factors.

Conclusion: Elevated SII concentrations correlated significantly with this mortality rate. The interpretable XGBoost model accurately detected the precise link between admission SII measurements and subsequent 28-day all-cause mortality in the target patient population.

Keywords: elderly patients, systemic immune-inflammation index, sepsis, community-acquired bacterial pneumonia, machine learning, prediction model

Introduction

Community-acquired pneumonia (CAP) remains a major cause of morbidity and mortality worldwide, imposing a substantial healthcare burden in China, with a reported incidence in China ranging from 29.8 to 221.0 per 10,000 hospital admissions.[1] Among hospitalized patients, bacterial pathogens account for a substantial proportion of severe cases. A frequent and life-threatening complication of CAP is sepsis, defined according to Sepsis-3 criteria as infection-associated organ dysfunction resulting from a dysregulated host response. Approximately one-third of sepsis patients with CAP progress to this critical state.[2]

Older adults are particularly vulnerable to poor outcomes. Advanced age is associated with impaired immune response, multiple comorbidities, and reduced physiological reserve, all of which contribute to increased susceptibility to severe

https://doi.org/10.2147/CIA.S560732
Received: 14 August 2025
Accepted: 12 March 2026
Published: 24 March 2026

infection and organ failure.[3] CAP is the leading cause of mortality among hospitalized patients with severe pneumonia, with the mortality rate in patients aged ≥65 years reaching 4.7%, which is the highest among all CAP cases,[1] and it escalates dramatically to nearly 50% in those requiring ICU admission due to respiratory failure or shock.[4–6] In addition to short-term mortality, pneumonia and sepsis in the elderly are linked to prolonged functional decline and increased long-term mortality after discharge.[7] Despite this high-risk profile, prognostic assessment tools specifically evaluated in elderly ICU patients with sepsis secondary to community-acquired bacterial pneumonia (CABP) remain limited.

Currently, conventional scoring systems, including CURB-65, the Pneumonia Severity Index (PSI), SOFA, and APACHE II are routinely applied for initial severity assessment in CAP and sepsis. However, their discriminative performance for short-term mortality is modest, with AUC values generally around 0.65–0.66.[4,8,9] Importantly, these scoring systems were primarily derived from mixed adult populations and were not specifically designed for very elderly patients requiring intensive care. Age-related immune dysregulation, multimorbidity, and atypical clinical presentations in older adults may limit the accuracy of these models in this subgroup. For example, in patients aged ≥80 years with severe pneumonia, the AUCs of CURB-65 and PSI for mortality prediction were approximately 0.61 and 0.52, respectively, suggesting that conventional scoring systems may not fully capture risk heterogeneity in older individuals.[10]

In elderly patients, outcomes are further influenced by comorbidity burden and nutritional status. The Charlson Comorbidity Index (CCI) has been widely used to quantify comorbidity burden and has been associated with mortality in patients with pneumonia and sepsis.[11,12] Likewise, hypoalbuminemia and the C-reactive protein-to-albumin ratio (CAR) have been reported as predictors of adverse outcomes in elderly patients.[13] However, while these indicators reflect comorbidity burden or systemic inflammatory status, they may not fully capture the complex immune dysregulation that characterizes sepsis.[14]

In recent years, systemic inflammatory indices derived from routine blood tests have been explored as potential prognostic markers in sepsis. Calculated from neutrophil, lymphocyte, and platelet counts, SII is a cost-effective and available marker that integrates assessment of inflammation, immune dysfunction, and coagulation.[15] Compared with other indices such as the neutrophil-to-lymphocyte ratio (NLR) or platelet-to-lymphocyte ratio (PLR), SII has shown promising prognostic value in heterogeneous critically ill populations.[16] However, most available studies have included mixed sepsis cohorts, and data focusing specifically on elderly patients with CABP-related sepsis are scarce. Notably, emerging evidence suggests that a J-shaped relationship between SII and 28-day mortality has been observed, with both extremely high and low values linked to increased mortality risk, reflecting hyperinflammation on one end and immune suppression on the other.[17,18] Whether such a pattern exists for SII in elderly patients with CABP-induced sepsis has not been clearly defined.

Machine learning (ML) methods have been increasingly applied in prognostic modeling in critical care. Conventional scoring systems and regression models rely on predefined linear relationships and limited interaction terms, which may not fully capture the complex and potentially non-linear relationships among clinical variables in elderly patients with sepsis. By capturing complex, non-linear interactions among variables, ML can potentially improve prediction accuracy.[19] However, data focusing specifically on elderly ICU patients with sepsis secondary to community-acquired bacterial pneumonia remain limited. In addition, the role of SII within machine learning–based prognostic models has not been well characterized. The interpretability of machine learning models is also an important consideration for clinical application.

Therefore, this study aimed to evaluate the association between SII obtained on the first day of ICU admission and 28-day mortality in elderly ICU patients with sepsis secondary to CABP, with particular attention to potential non-linear effects. We further developed a machine learning–based model including SII and routinely collected clinical variables and compared its performance with established severity scores and other inflammatory indicators. Given the single-center nature of the cohort and reliance on internal validation, further external validation in independent populations will be necessary to confirm the generalizability of the findings.

Materials and Methods

Study Design and Data Source

We conducted a retrospective cohort study for the development and internal validation of a multivariable prediction model. Clinical records of elderly patients admitted to the comprehensive ICU and EICU at Beijing Shijitan Hospital, Capital Medical University, between January 2020 and December 2024 were reviewed. For internal

validation, model development was performed in the EICU cohort, and performance was evaluated in the comprehensive ICU cohort from the same institution. This setting-based split (EICU vs ICU; approximately 7:3) was prespecified to provide a pragmatic assessment of model transportability across different ICU units within the hospital. Ethical approval was granted by the hospital's Ethics Committee (Approval No.: IIT2025-023-001). Due to the retrospective, non-interventional, and non-invasive character of this retrospective study, written informed consent requirements were waived. This retrospective study was not registered in any public registry. The study was conducted per the approved study protocol, complying with the ethical rules in the Declaration of Helsinki. The study was reported in accordance with the Transparent Reporting of a Multivariable Prediction Model for Individual Prognosis or Diagnosis (TRIPOD) statement to enhance methodological transparency.[20] (Table S5).

Inclusion and Exclusion Criteria

All patients meeting the following criteria were included: ≥ 65 years; All enrolled patients met the Sepsis-3.0 criteria (The Third International Consensus Definitions for Sepsis and Septic Shock) and the diagnostic criteria outlined in the Chinese Guidelines for the Diagnosis and Treatment of Adult Community-Acquired Pneumonia (2016 Edition); All subjects had complete clinical data. Exclusion criteria were: Hospitalization duration was less than 24 hours or death occurred within 24 hours of admission; Concurrent viral or fungal pneumonia; Critically ill patients who discontinued treatment (eg., withdrew from care) or whose 28-day survival status was unverifiable; Terminal-stage conditions involving fatal primary diseases, such as acute-phase myocardial infarction or cerebral hemorrhage; Hematologic disorders including granulocyte deficiency, aplastic anemia, or acute leukemia; HIV-positive status; documented autoimmune disorders; presence of severe immunocompromised conditions; or receipt of current immunosuppressive treatment regimens; Concurrent infections at other anatomical sites or acute/chronic inflammatory conditions; History of splenectomy or hypersplenia.

Clinical Data Collection

Patient data were obtained from the hospital's electronic medical record system, including age, gender, comorbidities (cardiovascular disease, hypertension, diabetes, chronic lung diseases (eg., COPD, bronchiectasis, bronchial asthma, lung cancer, and tuberculosis). Other comorbidities include renal disease, hepatic disease, cerebrovascular disease, and history of non-active malignancies), vital signs and laboratory parameters within 24 hours of admission, as well as bacterial microbiological test results within 48 hours of admission. SII was then calculated using the formula: SII = Platelets × Neutrophils / Lymphocytes.

Outcome and Primary Predictor

The investigation's primary outcome was 28-day all-cause mortality. SII served as the key predictor variable. Continuous predictor variables are retained in their original scale during model construction unless otherwise specified; categorical variables are coded as binary variables or dummy variables as appropriate. Nonlinearity was examined using restricted cubic splines. When a significant nonlinear association was observed, SII was categorized into quartiles to enhance clinical interpretability.

Sample Size Consideration

Although this was a retrospective cohort study without a pre-specified prospective power calculation, we assessed the adequacy of the available sample for prediction model development following the framework proposed by Riley et al[21] Based on 12 candidate predictors, an observed mortality rate of 21.4%, and an anticipated Cox–Snell R^2 of 0.10, the estimated minimum sample size required to ensure a shrinkage factor ≥0.9 was approximately 500 patients.[22]

Our cohort included 364 patients with 78 events, which falls slightly below this estimated threshold and suggests a potential risk of model overfitting under conventional regression frameworks. However, recent methodological research indicates that shrinkage factors ≥0.9 can still be achieved with lower event-per-parameter ratios when rigorous feature selection and penalized/regularized estimation methods are employed.[23] To address the sample size limitation, we applied dimensionality reduction, regularized machine learning algorithms, and cross-validation within the training dataset to

mitigate optimism and enhance generalizability. The model is therefore interpreted as exploratory, and external validation in larger multicenter cohorts is warranted.

Statistical Analysis

The data were analyzed using R software (v4.4.1, 2024–06-14 ucrt).[24] Variables containing less than 20% missing values underwent multiple imputation. According to the 28-day survival outcome, participants were classified into survivor and non-survivor groups. The SII was categorized into categorical variables based on quartiles. Normally distributed continuous measures were represented as arithmetic mean with standard deviation (mean ± standard deviation (SD)) and analyzed using independent-samples t-tests. Non-normally distributed continuous variables were presented in terms of median with interquartile range (IQR) and compared via Mann–Whitney *U*-tests. Categorical variables were reported as frequencies and percentages n (%), with intergroup comparisons employing the x^2 test or Fisher's exact test. The logistic regression model was used to evaluate the odds ratio (OR) of event occurrence and the 95% confidence interval. Restricted cubic splines (RCS) incorporated within regression frameworks were used to examine nonlinear SII-mortality associations. We selected the model with 3–7 knots by minimizing Akaike information criterion values. The statistical significance threshold was set at $P < 0.05$.

Missing Data Handling

Missing data were handled using multiple imputation by chained equations (MICE) with random forest algorithms implemented in R. We first assessed the missing data mechanism using Little's MCAR test, which did not reject the MCAR assumption ($\chi^2 = 3603$, df= 5093, p> 0.05).

Five imputed datasets were generated using random forest imputation with 50 iterations each to ensure convergence. The optimal imputed dataset was selected based on the minimum Akaike Information Criterion (AIC) value from logistic regression models. To validate the imputation quality, we compared the distribution of imputed values with the original complete data using Kolmogorov–Smirnov tests for continuous variables and chi-square tests for categorical variables. All variables showed no significant distributional differences (all $p > 0.1$), confirming the validity of the imputation procedure. Sensitivity analyses were conducted across all imputed datasets to ensure the robustness of our findings.

Model Development and Internal Validation

We chose the Boruta algorithm to filter pivotal predictive variables in the dataset. Boruta is a feature selection algorithm that creates copies of and shuffles all real features, obtaining the Z-score for each feature via a random forest model. At the same time, the algorithm generates shadow features by randomly shuffling copies of each real feature, and then obtains their corresponding Z-scores. It filters important features by comparing the Z-scores of each real feature with those of the shadow features. When the Z-scores of a specific real feature are significantly higher than those of the shadow features across multiple independent tests, that real feature is recognized as an important feature (green zone). Otherwise, it is classified as an unimportant feature (red zone). This process is repeated iteratively to identify the optimal variables.[25] After that, the selected variables were subsequently incorporated into multiple modeling approaches, including logistic regression, gradient boosting machine (GBM), random forest (RF), LightGBM, and XGBoost. All feature selection and model training procedures were performed exclusively in the EICU cohort, and model performance was subsequently evaluated in the ICU cohort.

Receiver operating characteristic (ROC) curves and their corresponding area under the curve (AUC) values were used to compare the predictive performance of the various models. Calibration was assessed using calibration plots and the Brier score. Decision curve analysis (DCA) was used to evaluate clinical utility. SHAP analysis was utilized for visual interpretation. SHAP values explain the extent to which each feature contributes to the model's predictive performance, and feature importance plots rank feature importance based on the average absolute value of SHAP values. SHAP was also used to visualize and analyze individual model predictions as outcomes of feature contributions.

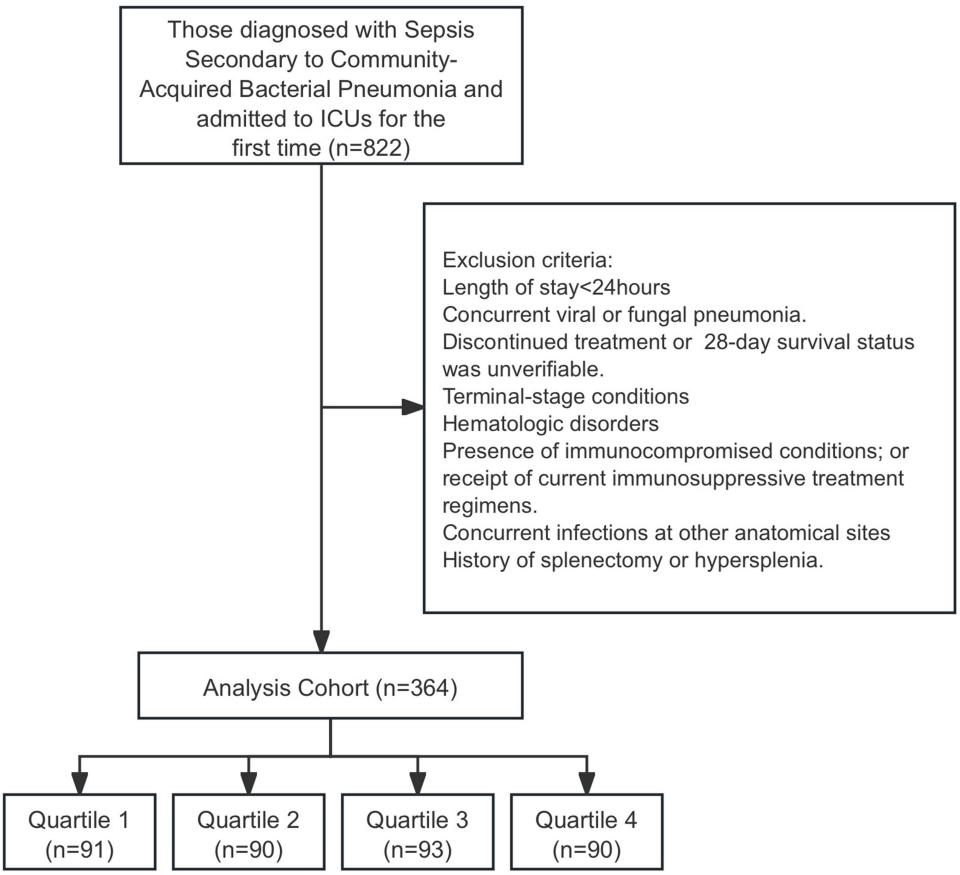

Figure 1 Flowchart of screening.

Results

This investigation incorporated clinical records from 364 eligible participants (Figure 1). Baseline demographic and clinical characteristics for the entire cohort are presented in Table 1, with a comparison between the training and test sets provided in (Table S1). A total of 26 variables had missing data, with missing rates ranging from 1% to 5%. Little's MCAR test indicated that the missing data pattern was consistent with MCAR ($p > 0.99$). After multiple imputation using random forests, the optimal imputed dataset (AIC = 181.20) was selected for primary analyses. Distribution consistency tests showed no significant differences between imputed and original data for all variables (all $p > 0.1$), validating our

Table 1 Baseline Characteristics of the Study Population

Variables	Total (n = 364)	Survival (n = 286)	Non-survival (n = 78)	P- value
Demographics				
Age	86.00 (80.00, 90.00)	85.00 (79.00, 90.00)	88.00 (83.00, 92.00)	0.002
Gender, n (%)				<0.001
Female	146 (40.1)	128 (44.8)	18 (23.1)	
Male	218 (59.9)	158 (55.2)	60 (76.9)	
Vital signs				
Heart Rate	88.00 (78.00, 103.00)	88.00 (78.00, 103.00)	90.00 (76.00, 105.00)	0.961
Respiratory Rate	21.00 (18.00, 26.00)	20.50 (18.00, 26.00)	21.00 (18.00, 27.75)	0.658
MAP	89.00 (78.58, 99.42)	89.83 (80.33,99.92)	84.83 (74.83,96.58)	0.021

(*Continued*)

Table 1 (Continued).

Variables	Total (n = 364)	Survival (n = 286)	Non-survival (n = 78)	P- value
Comorbidities, n (%)				
Hypertension	252 (69.2)	204 (71.3)	48 (61.5)	0.128
Coronary artery disease	84 (23.1)	70 (24.5)	14 (18.0)	0.289
Other cardiac disease	67 (18.4)	52 (18.2)	15 (19.2)	0.962
Chronic respiratory disease	220 (60.4)	161 (56.3)	59 (75.6)	0.003
Cerebrovascular disease	148 (40.7)	112 (39.2)	36 (46.2)	0.325
Other chronic neurological disease	52 (14.3)	38 (13.3)	14 (18.0)	0.39
Diabetes	133 (36.5)	99 (34.6)	34 (43.6)	0.185
Chronic kidney disease	52 (14.3)	40 (14.0)	12 (15.4)	0.896
Cancer	30 (8.2)	23 (8.0)	7 (9.0)	0.974
Disease severity scores				
SOFA	4 (2, 6)	3 (2, 5)	6 (3, 8)	< 0.001
APACHE II	14 (10, 21)	12 (9, 18)	22 (16, 27)	< 0.001
CURB-65	2 (2, 3)	2 (1.25, 3)	3 (3, 4)	< 0.001
PSI	40 (20, 60)	30 (10, 50)	70 (42.5, 90)	< 0.001
CCI	6 (5, 7)	6 (5, 7)	6 (5, 7)	0.089
Laboratory values				
WBC	9.53 (7.18, 13.24)	9.30 (7.07, 12.86)	11.43 (7.96, 14.54)	0.017
LYM	0.86 (0.54, 1.29)	0.90 (0.60, 1.39)	0.58 (0.33, 0.90)	< 0.001
MON	0.53 (0.37, 0.74)	0.54 (0.37, 0.77)	0.48 (0.35, 0.68)	0.257
NEU	8.00 (5.56, 11.46)	7.56 (5.26, 11.05)	10.28 (6.68, 13.16)	< 0.001
PLT	194.00 (149.00, 260.00)	192.50 (149.50,244.75)	212.50 (148.25,288.75)	0.054
ALT	16.00 (11.00, 27.00)	17.00 (11.00, 27.00)	14.00 (9.00, 23.50)	0.032
AST	20.00 (15.00, 32.00)	20.00 (15.00, 32.00)	20.00 (14.00, 32.00)	0.748
ALB	32.84 ± 5.54	33.56 ± 5.47	30.22 ± 5.00	< 0.001
Scr	85.50 (63.00, 120.25)	77.50 (60.25, 112.75)	109.00 (71.25, 155.50)	< 0.001
BUN	8.54 (6.04, 12.88)	8.10 (5.87, 12.32)	9.80 (7.01, 16.22)	0.01
CRP	51.92 (15.47,129.24)	44.74 (14.23,120.48)	101.38 (28.55,166.33)	< 0.001
PCT	0.17 (0.07, 1.03)	0.14 (0.07, 0.69)	0.52 (0.16, 2.85)	< 0.001
Microbial, n (%)				0.001
No microbiological documentation	163 (44.8)	142 (49.7)	21 (26.9)	
Gram-positive bacteria only	131 (36.0)	90 (31.5)	41 (52.6)	
Gram-negative bacteria only	22 (6.0)	16 (5.6)	6 (7.7)	
Polymicrobial infection	48 (13.2)	38 (13.3)	10 (12.8)	
SII category, n (%)				< 0.001
Quartile 1	91 (25.0)	81 (28.3)	10 (12.8)	
Quartile 2	90 (24.7)	85 (29.7)	5 (6.4)	
Quartile 3	93 (25.6)	77 (26.9)	16 (20.5)	
Quartile 4	90 (24.7)	43 (15.0)	47 (60.3)	
CAR	1.55 (0.42, 3.89)	1.32 (0.38, 3.49)	3.28 (0.82, 5.66)	< 0.001
PNI	32.76 ± 5.80	33.45 ± 5.82	30.23 ± 5.00	< 0.001

Abbreviations: SOFA, Sequential Organ Failure Assessment; APACHE II, Acute Physiology and Chronic Health Evaluation II; PSI, Pneumonia Severity Index; WBC, white blood cell count; NEU, neutrophil; LYM, lymphocyte; MON, monocyte; NEU, neutrophil; PLT, platelet; ALT, Alanine Aminotransferase; AST, Aspartate Aminotransferase; Scr, Serum Creatinine; BUN, blood urea nitrogen; CRP, C-reactive protein; PCT, procalcitonin; SII, platelets × neutrophils/lymphocytes; Quartile 1 (71.232–980.998), Quartile 2 (980.998–1954.254), Quartile 3 (1954.254–3497.984), Quartile4 (3497.984–35,047); CAR, C-reactive protein-albumin ratio; PNI, prognostic nutritional index.

imputation approach (Tables S2–S4, Figure S1 and S2). According to the baseline characteristics in Table 1, a total of 364 patients were included in this study, including 286 in the survival group and 78 in the non-survival group. The two groups showed significant differences in multiple dimensions. In terms of demographic characteristics, the median age of patients in the non-survival group was higher (88 vs 85 years, P=0.002), and the proportion of males was significantly

higher (76.92% vs 55.24%, P<0.001). Comorbidity analysis showed that the prevalence of chronic respiratory disease was significantly higher in the non-survival group (75.64% vs 56.29%, P=0.003), and there was no significant difference between the two groups for other comorbidities. In terms of disease severity scores, the SOFA, APACHE II, CURB-65 and PSI scores of the non-survival group were significantly higher than those in the survival group (all P<0.001), but the Charlson Comorbidity Index (CCI) was similar between the two groups. The SII was grouped by quartiles and converted into categorical variables: the first quartile (71.232 ≤ SII < 980.998), the second quartile (980.998 ≤ SII < 1954.254), the third quartile (1954.254 ≤ SII < 3497.984), and the fourth quartile (3497.984 ≤ SII ≤ 5047). The derivative index SII and C-reactive protein/albumin ratio (CAR) were significantly increased in the non-survival group, while the prognostic nutritional index (PNI) was significantly decreased (all P<0.001), which further confirmed that the patients in the non-survival group had more severe inflammatory response and malnutrition. In conclusion, non-survivors were mostly male, of advanced age, and exhibited higher disease severity scores, higher inflammation levels and more significant liver and kidney insufficiency.

Clinical Outcomes

Regarding the 28-day mortality rate, we can roughly observe from the baseline table that the mortality rate in the fourth quartile of SII was higher (Table 1). For further evaluation, we conducted univariate and multivariate logistic regression model analyses (Table 2) and found that when the first quartile of SII was used as the reference, the mortality rate in the fourth quartile increased significantly (OR 7.87, 95% CI:2.29–27.02, P = 0.001).

Restricted Cubic Spline (RCS)

According to RCS analysis (Figure 2), there was a significant U-shaped association between SII and the patient's 28-day all-cause mortality rate ($\chi 2$ = 57.8, P < 0.001). The lowest point of the RCS curve corresponds to an SII value of approximately 1267 (OR = 0.721, 95% CI: 0.581–0.895), which represents the lowest risk of mortality. The risk increases both below and above this threshold.

Boruta Algorithm

Figure 3 presents Boruta algorithm-based feature selection outcomes. The variables in green denote significant predictors, whereas red indicates unimportant features. The important features finally selected are sorted by Z-score as follows: SII, APACHE II, PSI, CURB-65, SOFA, ALB, PNI, age, PCT, CAR, Scr and gender.

Establishment and Validation of the Prediction Model

In order to predict the 28-day mortality rate of elderly patients with sepsis secondary to CABP, we selected five machine learning algorithms, including GBM, LR, RF, LightGBM and XGBoost. The variables were obtained through Boruta feature selection.

Figure 4 and Table 3 show the ROC curves of these models, with AUC values quantifying their performance. The XGBoost model achieved optimal discrimination capacity (training set: 0.901, 95% CI: 0.853–0.949; test set: 0.892, 95% CI: 0.820–0.964). It showed high sensitivity (0.839) and specificity (0.846). Subsequent model rankings were GBM (training set: 0.906, test set: 0.882), LightGBM (training set: 0.918, test set: 0.854), RF (training set: 0.895, test set: 0.857), and LR (training

Table 2 Logistic Regression Model (28-Day All-Cause Mortality)

SII	Univariable OR (95% CI)	*P*	Multivariable OR (95% CI)	*P*
Quartile 1	Reference	–	Reference	–
Quartile 2	0.48 (0.12–2.02)	0.320	0.59 (0.12–2.99)	0.525
Quartile 3	2.49 (0.88–6.99)	0.084	2.18 (0.60–7.90)	0.236
Quartile 4	10.33 (3.94–27.08)	<0.001	7.87 (2.29–27.02)	0.001

Notes: Quartile 1 (71.232–980.998), Quartile 2 (980.998–1954.254), Quartile 3 (1954.254–3497.984), Quartile4 (3497.984–35,047).
Abbreviation: SII, systemic immune-inflammation index.

https://doi.org/10.2147/CIA.S560732

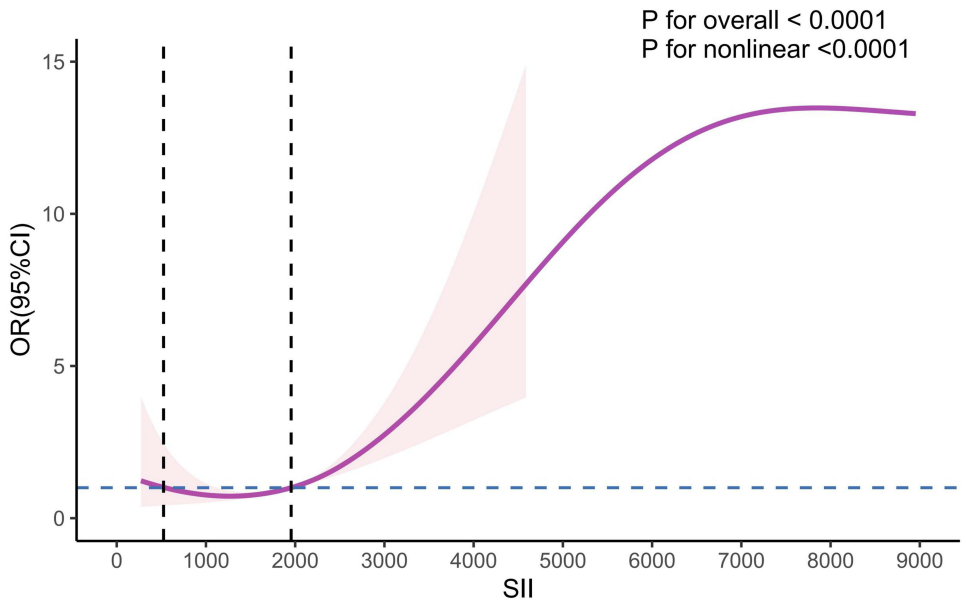

Figure 2 Restricted cubic spline (RCS) showing the association between SII and 28-day all-cause mortality. The solid line represents the adjusted odds ratio, with the shaded area indicating the 95% confidence interval.

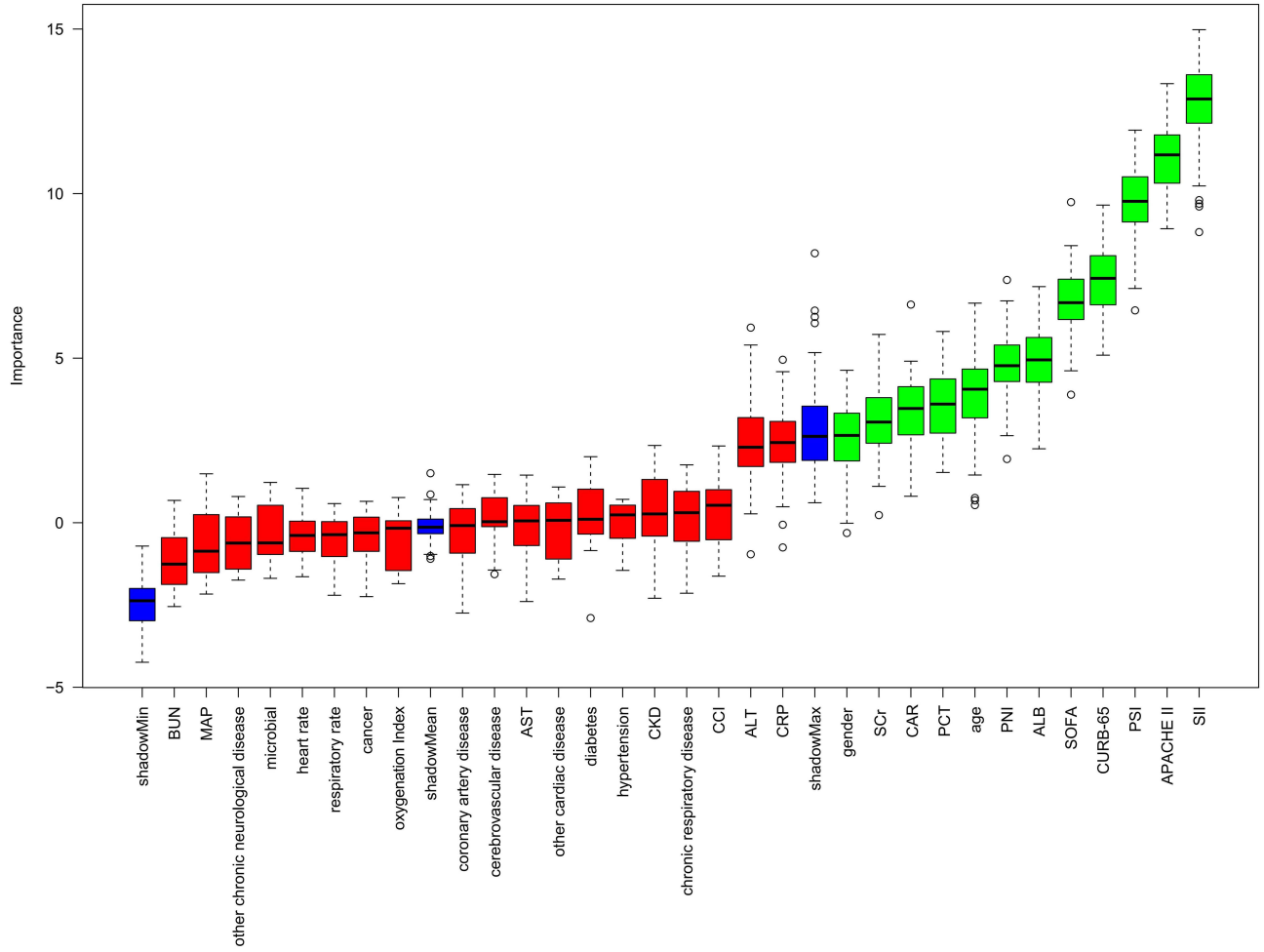

Figure 3 Feature selection utilizing the Boruta algorithm. The x-axis identifies variable names; the y-axis quantifies corresponding Z-scores. Boxplots visualize each variable's Z-score distribution, with green boxes representing significant predictive variables and red boxes non-significant ones.

https://doi.org/10.2147/CIA.S560732

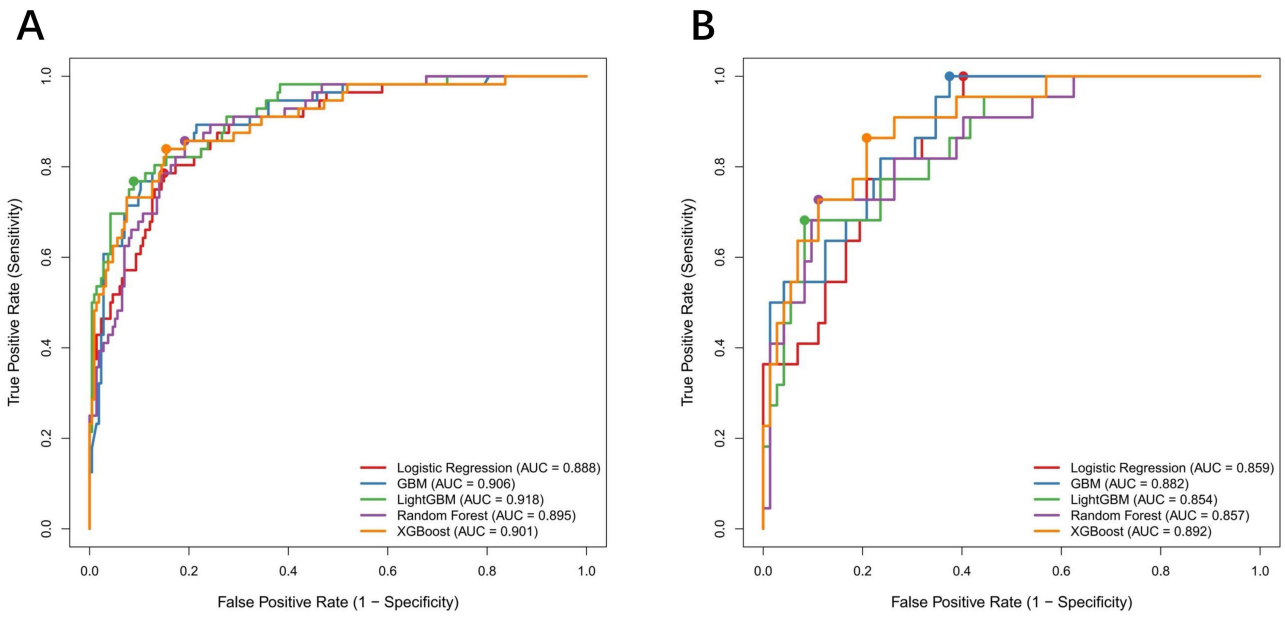

Figure 4 Comparison set of the area under the receiver operating curve. Performance evaluated by machine learning methods. (**A**): Comparison internal training set of the area under the receiver operating curve. (**B**): Comparison internal test set of the area under the receiver operating curve.
Abbreviations: XGBoost, extreme gradient boosting; SVM, support vector machine; RF, random forest; GLM, Generalized Linear Model; LightGBM, Light Gradient Boosting Machine.

set: 0.888, test set: 0.859). Calibration performance was evaluated using calibration plots (Figure 5), Brier scores, and calibration error metrics (ECE and MCE) (Table 4). In the validation cohort, the XGBoost model demonstrated the lowest Brier score (0.110) and the lowest expected calibration error (ECE = 0.066), indicating the most favorable agreement between predicted probabilities and observed outcomes. The DCA (Figure 6) suggests that the models provide a large net benefit across all models. Within the defined probability thresholds, XGBoost generated the greatest clinical net benefit. The machine learning algorithms were used to evaluate the 28-day mortality risk of elderly patients with sepsis secondary to CABP, which may facilitate early intervention to improve their short-term outcomes, indicating that the model has stable clinical utility.

XGBoost ML Model Performance Evaluation

The SHAP summary plot illustrates the correlation between all features in the XGBoost model and the 28-day all-cause mortality rate of elderly sepsis patients secondary to CABP (Figure 7A). The figure displays the 12 most important variables included in the model, ranked by importance. The X-axis, representing SHAP values, serves as a consistency metric to evaluate the impact of features on the model. The ordering of features on the Y-axis reflects their importance in the prediction model. In each row of the feature importance plot, all feature attributes related to the outcome are visually presented, with orange data points indicating high values and purple data points indicating low values. SHAP values

Table 3 Model Discrimination Performance on Training and Test Sets

Model	Training set				Test set			
	AUC	95% CI	Sensitivity	Specificity	AUC	95% CI	Sensitivity	Specificity
XGBoost	0.901	0.853–0.949	0.839	0.846	0.892	0.820–0.964	0.864	0.792
GBM	0.906	0.862–0.951	0.839	0.846	0.882	0.811–0.953	1.000	0.625
LightGBM	0.918	0.878–0.958	0.768	0.911	0.854	0.767–0.942	0.682	0.917
RF	0.895	0.852–0.939	0.857	0.808	0.857	0.768–0.946	0.727	0.889
LR	0.888	0.842–0.935	0.786	0.850	0.859	0.783–0.935	1.000	0.597

Abbreviations: AUC, area under curve; CI, Confidence Interval; XGBoost, extreme gradient boosting; GBM, Gradient Boosting Machine; LightGBM, Light Gradient Boosting Machine; RF, random forest; LR, Logistic Regression.

https://doi.org/10.2147/CIA.S560732

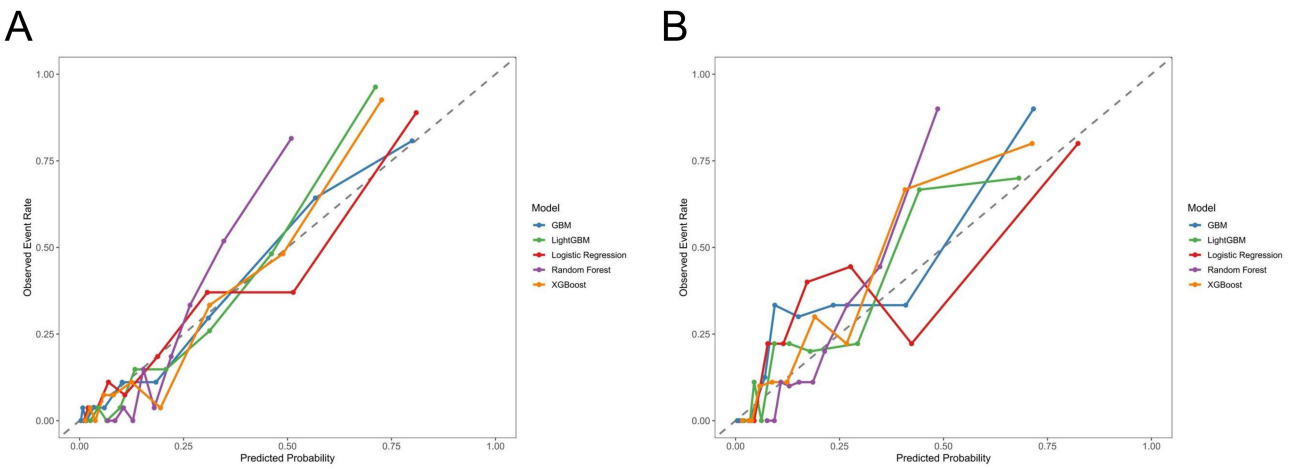

Figure 5 Calibration curves of the model. (**A**) Training set; (**B**) Test set. The diagonal dashed line represents perfect prediction, where predicted probabilities match observed outcomes. The solid line shows model performance; closer fit to the diagonal indicates better calibration.

exceeding zero correlate positively with mortality risk, and this risk rises as the SHAP value increases. The risk of death increases as the values of the following factors rise: SII, APACHE II, age, PSI, gender, SCr, PNI, ALB, CURB-65. To further clarify the most important characteristic factors in the prediction model, the SHAP importance plot shows that SII is the strongest predictor of 28-day mortality in elderly patients with sepsis secondary to CABP. The order from highest to lowest importance is as follows: APACHE II, age, PSI, gender, Scr, PNI, ALB and CURB-65 (Figure 7B). To demonstrate how the XGBoost model evaluates the contribution of features for individual patients, we used SHAP force plot to explain the predictions for two patients. Features promoting adverse outcomes appear in red, while protective factors are rendered blue. Bar lengths quantitatively reflect contribution intensity. Figure 7C shows an example of a patient with poor prognosis. Red features contributed to an increased risk of mortality, which exceeds the model's average predicted value. In this case, the patient was predicted to be at high risk of death due to elevated inflammation indicators (SII), elevated disease severity scores (SOFA, APACHE II, CURB-65, PSI), worse nutritional status (ALB, PNI), and organ dysfunction (SCr). The example in Figure 7D is a survivor, with relatively low disease severity scores (SOFA, APACHE II, PSI) and SII.

Discussion

In this single-center, five-year retrospective study, we constructed an interpretable machine learning model to explore SII's relationship with 28-day all-cause mortality in geriatric patients with sepsis secondary to CABP. After comparing the performance of five machine learning models, we found that the XGBoost model performed best, so we chose this

Table 4 Calibration Metrics for Machine Learning Models on Training and Test Sets

Model	Training Set			Test Set		
	ECE	MCE	Brier	ECE	MCE	Brier
XGBoost	0.049	0.199	0.091	0.066	0.259	0.110
LightGBM	0.057	0.251	0.088	0.072	0.225	0.121
GBM	0.026	0.076	0.089	0.086	0.239	0.116
RF	0.108	0.306	0.115	0.093	0.414	0.134
LR	0.040	0.143	0.099	0.094	0.228	0.124

Abbreviations: ECE, Expected Calibration Error; MCE, Maximum Calibration Error; XGBoost, extreme gradient boosting; GBM, Gradient Boosting Machine; LightGBM, Light Gradient Boosting Machine; RF, random forest; LR, Logistic Regression.

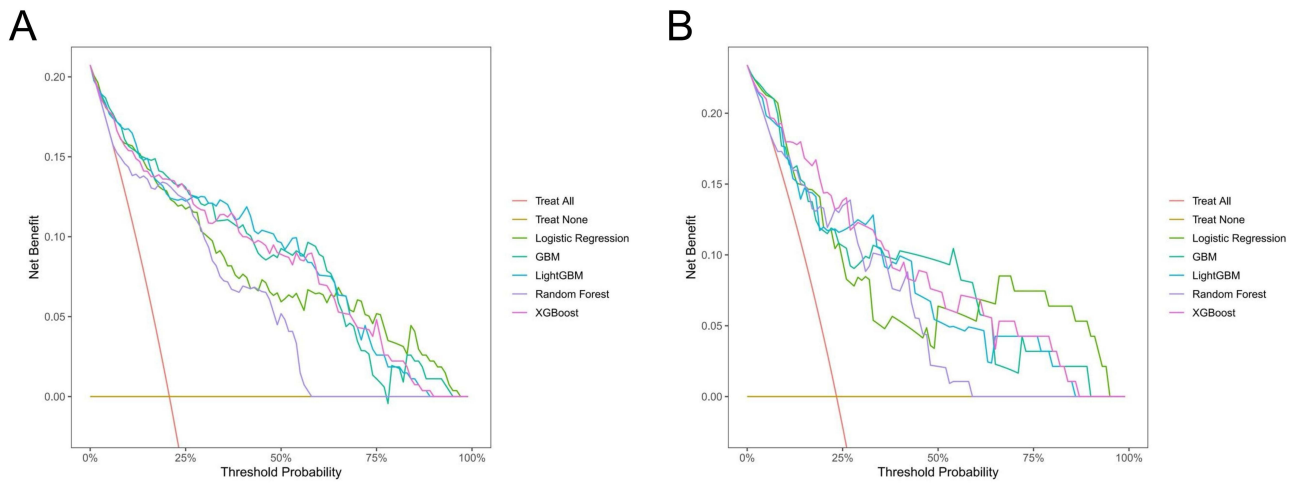

Figure 6 Decision curve analysis (DCA) of the five models. (**A**) Training set. (**B**) Test set.
Abbreviations: XGBoost, extreme gradient boosting; SVM, support vector machine; RF, random forest; GLM, Generalized Linear Model; LightGBM, Light Gradient Boosting Machine.

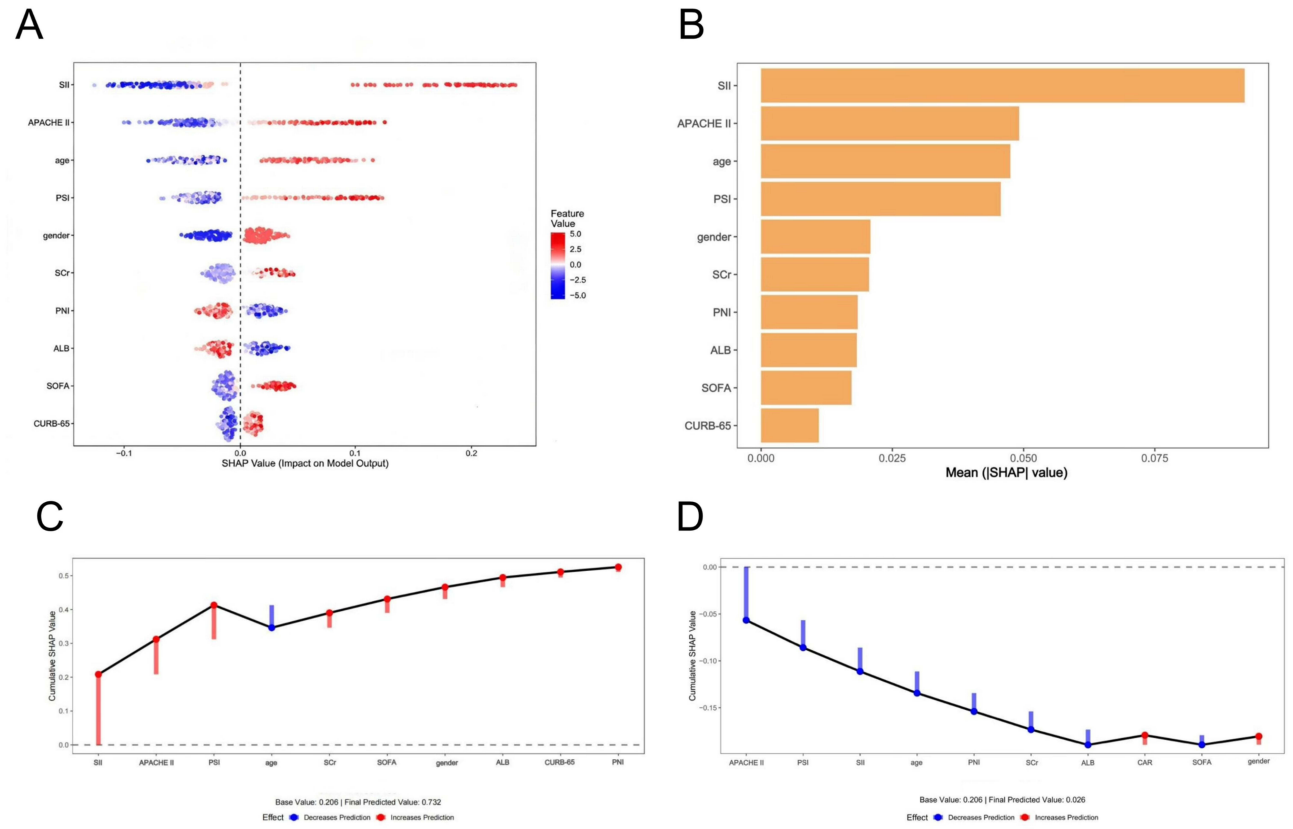

Figure 7 Feature importance analysis by SHAP method for XGBoost model. (**A**) SHAP summary plot. (**B**) feature importance. FIGURE 7C and 7D Force plots visualized individual model prediction as result of feature contributions. (**C**) A case with poor prognosis. (**D**) A case with favorable prognosis.

model for mortality prediction. During the process of screening important features and analyzing the predictive model performance, elevated SII levels at initial hospitalization significantly correlated with 28-day mortality. SHAP analysis suggested that SII was the most important feature in the XGBoost model as well. Through a search of existing relevant literature, we found no prior investigations examining SII's association with early adverse outcomes in this specific

https://doi.org/10.2147/CIA.S560732

patient population. Compared with previous studies that used SII to predict poor prognosis in sepsis patients, our research has certain novel aspects. Our research included five commonly used machine learning models and conducted a multi-model comparison. The results suggest that the machine learning models have ideal predictive discrimination. Decision curve analysis confirming XGBoost's maximal clinical net benefit within defined probability thresholds.

As one of the most important infectious causes of sepsis, CAP has a fatality rate comparable to that of acute myocardial infarction.[26,27] Thus, early identification and intervention for the disease are crucial. Sepsis fundamentally manifests as dysregulated host response to infection and an immune disorder, so monitoring the patient's immune function may have certain implications for the severity and prognosis of the disease.[28] In the severe sepsis stage, the expression of the anti-apoptotic protein myeloid cell leukemia-1 (Mcl-1) is upregulated, which inhibits neutrophil apoptosis and leads to their overactivation. This causes tissue damage to the body and induces inflammatory storms.[29] Therefore, neutrophil apoptotic rates exhibit an inverse correlation with sepsis severity, serving as potential biomarkers for clinical assessment.[30] In addition, patients with severe sepsis usually have both an inflammatory response and an immunosuppressive state. The degree of lymphocyte reduction can reflect the extent of immunosuppression in sepsis, and persistent lymphocytopenia is associated with a poor prognosis in patients with sepsis.[31,32] Platelets are among the first cells to arrive at sites of infection and inflammation. The interaction between them and immune cells plays an important role in immunomodulation and the clearance of inflammatory factors.[33] Under the stimulation of sepsis, platelets capture and kill pathogens such as *Staphylococcus aureus* and *Escherichia coli* by inducing neutrophils to release neutrophil extracellular traps (NETs). At the same time, bacterial toxins cause platelet destruction.[34] Coagulation dysfunction, poor activation of platelets, and immune destruction during sepsis can lead to excessive platelet depletion and dysfunction.[35] Some studies have pointed out that the rapid and continuous decline in platelet count is an important predictor of adverse sepsis outcomes.[36] On this basis, the SII, which is derived from neutrophil, lymphocyte, and platelet counts, serves as a novel biomarker reflecting the integrated inflammatory, immunological, and coagulation pathway status.[37] Some research has proposed that elevated SII levels demonstrate a significant correlation with early poor prognosis in sepsis. In severe cases, infection-induced bone marrow suppression or immunosuppression establishes a J-curve association between SII and mortality risk, where both critically low and high SII values increase early death probability.[18,38] These findings align with our study's results regarding SII's U-shaped relationship with 28-day mortality in the target cohort.

The Boruta algorithm filters important features by simulating randomness and is currently a mature and widely used method.[39] Our application of this algorithm positioned SII within the green zone, achieving the maximal Z-score among selected the features. This outcome signifies SII's pivotal role in the present investigation and its strong association with short-term survival outcomes. In addition, logistic regression analysis further corroborated these findings, demonstrating a significant link between elevated SII levels and increased 28-day mortality risk in sepsis patients. After incorporating the important features selected through screening into various machine learning models, all models showed good predictive performance. Among the five machine learning classifiers, XGBoost exhibited optimal discriminative capacity, which was manifested through the highest AUC alongside elevated sensitivity and specificity metrics, establishing it as the baseline predictive framework.

The XGBoost algorithm constructs an ensemble model using base decision trees optimized for loss minimization. This methodology offers computational efficiency, superior generalization capability, and enhanced predictive accuracy. While efficiently handling missing data, it can combine multiple weak prediction models to form a more accurate prediction model.[19,40] Some previous sepsis-related studies have also emphasized that the XGBoost model has better predictive performance. Fan et al proposed that, compared with LR, RF, MLP, and SVC, XGBoost has the strongest predictive ability for the 7-day, 14-day, and 28-day prognosis of Sepsis-associated acute kidney injury (SA-AKI).[19] In addition, a meta-analysis summarized the comparison of 104 machine learning models and found that, in terms of predicting the prognosis of sepsis, the algorithmic approaches significantly outperform conventional clinical scoring systems in forecasting sepsis prognosis. XGBoost showed better predictive performance as well.[41]

The results of the interpretation and visual analysis of the XGBoost model using SHAP show that the most important characteristics are SII, APACHE II, age, PSI, gender, Scr, PNI, ALB, SOFA, and CURB-65. Therefore, the model not only elucidates the key features but also establishes a high-performance model for predicting mortality in elderly patients with sepsis secondary to CABP. At the same time, the findings of the SHAP analysis continue to support a significant and strong correlation between SII and the 28-day all-cause mortality rate in elderly patients with sepsis secondary to CABP.

In addition to SII, composite indices reflecting both inflammation and nutritional status have garnered increasing attention in critical care prognostication. Uluç et al recently demonstrated that the HALP score (hemoglobin, albumin, lymphocytes, and platelets) and the C-reactive protein/albumin ratio (CAR), composite indicators of inflammation and nutrition, are effective predictors of mortality in elderly patients in respiratory intensive care units.[42] Our study incorporated CAR alongside the Prognostic Nutritional Index (PNI) and Charlson Comorbidity Index. Except for the Charlson Comorbidity Index, CAR and PNI demonstrated significant differences between survivors and non-survivors (Table 1) and were identified as important features by the Boruta algorithm, consistent with the aforementioned findings. However, in the SHAP analysis of the optimal XGBoost model, SII remained the most influential predictor, surpassing CAR and PNI in importance. This may stem from SII's focus on sepsis's most critical pathophysiological mechanisms, integrating inflammatory (neutrophil), immune (lymphocyte), and coagulation (platelet) pathways. While CAR and PNI primarily capture inflammatory and nutritional interactions, their simultaneous inclusion in feature selection underscores the multifaceted nature of risk assessment in elderly sepsis patients.

Recent prospective studies have compared the predictive ability of SII with traditional severity scores. For instance, Nazik et al found that APACHE II remained a leading predictor of 28-day mortality in sepsis,[43] while Acar et al reported comparable predictive power between SII and CURB-65 (AUCs 0.737 vs. 0.773) in CAP patients.[44] However, in our study, based on the characteristic screening results of the Boruta algorithm and the analysis of the SHAP summary plot constructed by the machine learning model, SII was identified as the strongest indicator for 28-day mortality due to sepsis secondary to CABP in elderly patients, outperforming not only conventional inflammatory indicators (PCT, CRP), but also pneumonia severity scores (CURB-65, PSI), and general illness severity scores (SOFA, APACHE II). Furthermore, when SII was combined with PCT, PSI, and CURB-65, the XGBoost model achieved an AUC of 0.910, while the AUCs of the other models are greater than 0.88. This suggests a synergistic effect among SII, PCT, the pneumonia severity scores, and the disease severity scores. Leveraging SII's advantages, including ease of access, superior predictive ability, sensitivity, and specificity, the combined use of SII with traditional scoring systems and inflammatory indicators offers new insights for the early and rapid assessment of elderly critically ill patients in clinical practice. It also provides additional evidence for preventive strategies.

From a clinical perspective, integrating SII into existing risk stratification systems is theoretically feasible. While APACHE II has been validated as one of the most authoritative disease severity assessment systems, it requires comprehensive collection of disease-specific data. In contrast, SII values at admission can be rapidly obtained through routine complete blood count testing. Notably, the synergistic effect observed when combining SII with traditional scores (AUC 0.910) indicates complementary assessment of disease risk dimensions: APACHE II reflects physiological dysfunction, while SII emphasizes immune-inflammatory dysregulation. However, at this exploratory stage, the core value of this model lies not in immediate clinical application but in demonstrating the potential for integrating SII with conventional variables to enhance prognostic prediction. Prospective, multicenter validation remains essential before any practical implementation.

This study has several limitations that should be acknowledged. First, its retrospective, single-center design limits the generalizability of the findings to other settings and ethnic groups. Additionally, this design introduces potential risks of selection bias and unmeasured confounding factors. Second, and crucially, our model was developed and validated only internally. The lack of external validation in an independent cohort represents the major limitation in terms of its clinical translatability and robustness. Other limitations include a modest sample size, which may restrict the statistical power for subgroup analyses, as well as the use of data imputation. Although we used multiple imputation for missing data, and tests suggested data were missing completely at random, imputation itself may introduce some degree of inaccuracy compared to an analysis based on a complete source dataset.

Given these limitations, the model should be regarded as exploratory research at this stage. Before any practical clinical application, rigorous prospective, multicenter external validation is required to confirm its predictive accuracy, calibration, and clinical utility across diverse settings. Future studies should also focus on collecting larger cohort data to conduct reliable sensitivity analyses and evaluate the model's performance as a decision support tool in clinical practice.

Conclusion

In short, a nonlinear U-shaped relationship was observed between admission-day SII levels and 28-day all-cause mortality among geriatric patients with sepsis secondary to CABP. Elevated SII values demonstrated a significant positive correlation with early detrimental outcomes. Machine learning methodologies provide reliable prognostic predictions for adverse events

in this population. Among the evaluated algorithms, XGBoost exhibited optimal efficacy, with SII identified as its pivotal predictive feature. Consequently, SII represents a viable biomarker for forecasting adverse clinical endpoints in elderly patients with sepsis secondary to CABP, although multicenter prospective validation remains warranted.

Abbreviations

SII, systemic immune-inflammation index; CABP, community-acquired bacterial pneumonia; CAP, community-acquired pneumonia; XGBoost, extreme gradient boosting; GBM, Gradient Boosting Machine; LightGBM, Light Gradient Boosting Machine; RF, random forest; LR, Logistic Regression; AUROC, area under the receiver operating characteristic curve; AUC, area under the curve; ROC, receiver operating characteristic; *ECE*, Expected Calibration Error; *MCE*, Maximum Calibration Error; DCA, decision curve analysis; SHAP, SHapley Additive exPlanations; SOFA, sequential organ failure assessment; APACHE II, acute physiology and chronic health evaluation II; PSI, pneumonia severity index; PCT, procalcitonin; BUN, blood urea nitrogen; Mcl-1, myeloid cell leukemia-1; NETs, neutrophil extracellular traps; SA-AKI, sepsis-associated acute kidney injury.

Data Sharing Statement

The datasets and code generated and/or analyzed during the current study are available from the corresponding author upon reasonable request.

Funding

This work was supported by the 2022 Beijing Major Epidemic Prevention and Control Key Speciality Intensive Care Medical Construction Project (Grant No. ZDYQFZZDZK).

Disclosure

The authors report no conflicts of interest in this work.

References

1. Zhu YG, Tang XD, Lu YT, Zhang J, Qu JM. Contemporary situation of community-acquired pneumonia in china: a systematic review. *J Transl Int Med*. 2018;6(1):26–31. doi:10.2478/jtim-2018-0006
2. Matthay MA, Arabi YM, Siegel ER, et al. Phenotypes and personalized medicine in the acute respiratory distress syndrome. *Intensive Care Med*. 2020;46(12):2136–2152. doi:10.1007/s00134-020-06296-9
3. Garcia-Carretero R, Gil-Prieto R, Hernandez-Barrera V, et al. Epidemiological and clinical impact of pneumococcal disease in Spain in 2023: a nationwide retrospective analysis. *Hum Vaccin Immunother*. 2025;21(1):2579385. doi:10.1080/21645515.2025.2579385
4. Naghavi M, Abajobir AA, Abbafati C. GBD 2016 causes of death collaborators. global, regional, and national age-sex specific mortality for 264 causes of death, 1980-2016: a systematic analysis for the global burden of disease study 2016. *Lancet*. 2017;390(10100):1151–1210. doi:10.1016/S0140-6736(17)32152-9
5. Lim WS, van der Eerden MM, Laing R, et al. Defining community acquired pneumonia severity on presentation to hospital: an international derivation and validation study. *Thorax*. 2003;58(5):377–382. doi:10.1136/thorax.58.5.377
6. Ferreira-Coimbra J, Sarda C, Rello J. Burden of community-acquired pneumonia and unmet clinical needs. *Adv Ther*. 2020;37(4):1302–1318. doi:10.1007/s12325-020-01248-7
7. Dick A, Liu H, Zwanziger J, et al. Long-term survival and healthcare utilization outcomes attributable to sepsis and pneumonia. *BMC Health Serv Res*. 2012;12:432. doi:10.1186/1472-6963-12-432
8. Myint PK, Kamath AV, Vowler SL, et al. The CURB (confusion, urea, respiratory rate and blood pressure) criteria in community-acquired pneumonia (CAP) in hospitalised elderly patients aged 65 years and over: a prospective observational cohort study. *Age Ageing*. 2005;34(1):75–77. doi:10.1093/ageing/afh234
9. Richards G, Levy H, Laterre PF, et al. CURB-65, PSI, and APACHE II to assess mortality risk in patients with severe sepsis and community acquired pneumonia in PROWESS. *J Intensive Care Med*. 2011;26(1):34–40. doi:10.1177/0885066610383949
10. Lv C, Pan T, Shi W, et al.Establishment of risk model for elderly CAP at different age stages: a single-center retrospective observational study.*Sci Rep*.13;1.12432. doi:10.1038/s41598-023-39542-3
11. Jouffroy, Ouffroy R, Gilbert B, et al. Relationship between prehospital modified Charlson Comorbidity Index and septic shock 30-day mortality. *Am J Emerg Med*. 2022;60:128–133. doi:10.1016/j.ajem.2022.08.003
12. Zan Y, Song W, Wang Y, et al. Nomogram for predicting in-hospital mortality of nonagenarians with community-acquired pneumonia. *Geriatr Gerontol Int*. 2022;22(8):635–641. doi:10.1111/ggi.14430
13. Capurso C, Lo Buglio A, Bellanti F, et al. C-reactive protein/albumin ratio vs. prognostic nutritional index as the best predictor of early mortality in hospitalized older patients, regardless of admitting diagnosis. *Nutrients*. 2025;17(17):2907. doi:10.3390/nu17172907
14. Zou J, Xiao Y, Zhang L, et al. Enhanced insights into immunity traits of elderly patients in the intensive care unit with infections: evidence from a multicenter, prospective observational study. *Crit Care*. 2025;29(1):386. doi:10.1186/s13054-025-05616-z

15. Mangalesh S, Dudani S, Malik A. The systemic immune-inflammation index in predicting sepsis mortality. *Postgrad Med*. 2023;135(4):345–351. doi:10.1080/00325481.2022.2140535
16. Zhu S, Zhou Q, Hu Z, et al. Assessment of neutrophil to lymphocyte ratio, platelet to lymphocyte ratio and systemic immune-inflammatory index, as diagnostic markers for neonatal sepsis. *J Int Med Res*. 2024;52(8):3000605241270696. doi:10.1177/03000605241270696
17. Sun J, Qi Y, Wang W, et al. Systemic immune-inflammation index (sii) as a predictor of short-term mortality risk in sepsis-associated acute kidney injury: a retrospective cohort study. *Med Sci Monit*. 2024;30:e943414. doi:10.12659/MSM.943414
18. Jiang D, Bian T, Shen Y, et al. Association between admission systemic immune-inflammation index and mortality in critically ill patients with sepsis: a retrospective cohort study based on MIMIC-IV database. *Clin Exp Med*. 2023;23(7):3641–3650. doi:10.1007/s10238-023-01029-w
19. Fan Z, Jiang J, Xiao C, et al. Construction and validation of prognostic models in critically Ill patients with sepsis-associated acute kidney injury: interpretable machine learning approach. *J Transl Med*. 2023;21(1):406. doi:10.1186/s12967-023-04205-4
20. Collins GS, Reitsma JB, Altman DG, et al. Transparent reporting of a multivariable prediction model for individual prognosis or diagnosis (TRIPOD): the TRIPOD statement. *BMJ*. 2015;350:g7594. doi:10.1136/bmj.g7594
21. Riley RD, Ensor J, Snell KIE, et al. Calculating the sample size required for developing a clinical prediction model. *BMJ*. 2020;368:m441. doi:10.1136/bmj.m441
22. Riley RD, Snell KI, Ensor J, et al. Minimum sample size for developing a multivariable prediction model: PART II - binary and time-to-event outcomes. *Stat Med*. 2019;38(7):1276–1296. doi:10.1002/sim.7992
23. Riley RD, Snell KIE, Martin GP, et al. Penalization and shrinkage methods produced unreliable clinical prediction models especially when sample size was small. *J Clin Epidemiol*. 2021;132:88–96. doi:10.1016/j.jclinepi.2020.12.005
24. Team RC. *R: A Language and Environment for Statistical Computing*. Vienna, Austria: R Foundation for Statistical Computing; 2025.
25. Yan F, Chen X, Quan X, et al. Association between the stress hyperglycemia ratio and 28-day all-cause mortality in critically ill patients with sepsis: a retrospective cohort study and predictive model establishment based on machine learning. *Cardiovasc Diabetol*. 2024;23(1):163. doi:10.1186/s12933-024-02265-4
26. Kolditz M, Ewig S, Klapdor B, et al. Community-acquired pneumonia as medical emergency: predictors of early deterioration. *Thorax*. 2015;70 (6):551–558. doi:10.1136/thoraxjnl-2014-206744
27. Shah RU, Henry TD, Rutten-Ramos S, et al. Increasing percutaneous coronary interventions for ST-segment elevation myocardial infarction in the United States: progress and opportunity. *JACC Cardiovasc Interv*. 2015;8(1 Pt B):139–146. doi:10.1016/j.jcin.2014.07.017
28. Nedeva C. Inflammation and cell death of the innate and adaptive immune system during sepsis. *Biomolecules*. 2021:11(7):1011. doi:10.3390/biom11071011
29. Zhang J, Shao Y, Wu J, et al. Dysregulation of neutrophil in sepsis: recent insights and advances. *Cell Commun Signal*. 2025;23(1):87. doi:10.1186/s12964-025-02098-y
30. Fialkow L, Fochesatto Filho L, Bozzetti MC, et al. Neutrophil apoptosis: a marker of disease severity in sepsis and sepsis-induced acute respiratory distress syndrome. *Crit Care*. 2006;10(6):R155. doi:10.1186/cc5090
31. Liu W, Tao Q, Xiao J, et al. Low lymphocyte to high-density lipoprotein ratio predicts mortality in sepsis patients. *Front Immunol*. 2023;14:1279291. doi:10.3389/fimmu.2023.1279291
32. Drewry AM, Samra N, Skrupky LP, et al. Persistent lymphopenia after diagnosis of sepsis predicts mortality. *Shock*. 2014;42(5):383–391. doi:10.1097/SHK.0000000000000234
33. Mandel J, Casari M, Stepanyan M, et al. Beyond hemostasis: platelet innate immune interactions and thromboinflammation. *Int J Mol Sci*. 2022;23 (7):3868. doi:10.3390/ijms23073868
34. Page MJ, Pretorius E. A champion of host defense: a generic large-scale cause for platelet dysfunction and depletion in infection. *Semin Thromb Hemost*. 2020;46(3):302–319. doi:10.1055/s-0040-1708827
35. Cox D. Sepsis - it is all about the platelets. *Front Immunol*. 2023;14:1210219. doi:10.3389/fimmu.2023.1210219
36. Ye Q, Wang X, Xu X, et al. Serial platelet count as a dynamic prediction marker of hospital mortality among septic patients. *Burns Trauma*. 2024;12:tkae016. doi:10.1093/burnst/tkae016
37. Braun LJ, Stegmeyer RI, Schäfer K, et al. Platelets docking to VWF prevent leaks during leukocyte extravasation by stimulating Tie-2. *Blood*. 2020;136(5):627–639. doi:10.1182/blood.2019003442
38. Ma K, Zhang Y, Hao J, et al. Correlation analysis of systemic immune inflammatory index, Serum IL-35 and HMGB-1 with the severity and prognosis of sepsis. *Pak J Med Sci*. 2023;39(2):497–501. doi:10.12669/pjms.39.2.6651
39. Yue S, Li S, Huang X, et al. Machine learning for the prediction of acute kidney injury in patients with sepsis. *J Transl Med*. 2022;20(1):215. doi:10.1186/s12967-022-03364-0
40. Cao S, Hu Y. Creating machine learning models that interpretably link systemic inflammatory index, sex steroid hormones, and dietary antioxidants to identify gout using the SHAP (SHapley Additive exPlanations) method. *Front Immunol*. 2024;15:1367340. doi:10.3389/fimmu.2024.1367340
41. Zhang Y, Xu W, Yang P, et al. Machine learning for the prediction of sepsis-related death: a systematic review and meta-analysis. *BMC Med Inform Decis Mak*. 2023;23(1):283. doi:10.1186/s12911-023-02383-1
42. Uluç K, Akkütük Öngel E, Çolakoğlu ŞM, et al. Effects of HALP score, c-reactive protein/albumin ratio, and platelet/lymphocyte ratio on predicting mortality in geriatric patients in the respiratory intensive care unit. *Clin Interv Aging*. 2025;20:815–823. doi:10.2147/CIA.S482214
43. Nazik S, Ates S, Seyithanoglu M, et al. Evaluation of serum ischemia-modified albumin and oxidative stress markers in patients with sepsis. *Infect Drug Resist*. 2025;18:5079–5086. doi:10.2147/IDR.S500446
44. Acar E, Gokcen H, Demir A, et al. Comparison of inflammation markers with prediction scores in patients with community-acquired pneumonia. *Bratisl Lek Listy*. 2021;122(6):418–423. doi:10.4149/BLL_2021_069